Journal of Inorganic Biochemistry 177 (2017) 27–38

Contents lists available at ScienceDirect

Journal of Inorganic Biochemistry

journal homepage: www.elsevier.com/locate/jinorgbio

In vitro anticancer activity of new gold(III) porphyrin complexes in colon cancer cells

Fatima Dandash[a], David Yannick Léger[a], Chloë Fidanzi-Dugas[a], Soumaya Nasri[a,b], Frédérique Brégier[a], Robert Granet[a], Walid Karam[c], Mona Diab-Assaf[c], Vincent Sol[a], Bertrand Liagre[a,*]

[a] Université de Limoges, LCSN, EA 1069, F-87000 Limoges, France
[b] Université de Monastir, Laboratoire de Physico-chimie des Matériaux, Faculté des Sciences de Monastir, Tunisie
[c] Molecular Tumorigenesis and Anticancer Pharmacology, EDST, Lebanese University, Hadath, Lebanon

ARTICLE INFO

Keywords:
Gold complexes
Porphyrin
Cancer
Apoptosis
Survival pathways

ABSTRACT

Colorectal cancer (CRC) is the third most common cancer diagnosed worldwide. The limitations of cisplatin-based chemotherapy have prompted intense interest among scientists to search for alternative metal-based anticancer medicines. Gold(III) complexes have been among the most widely investigated since they showed higher cytotoxicity than cisplatin and promising in vitro and in vivo anticancer activities in CRC but their clinical usefulness has been limited by their poor stability under physiological conditions. A novel gold(III) porphyrin complexes [gold(III) porphyrin-adamantane chloride (SN1) and gold(III) porphyrin mono-acetate chloride (SN2)] with improved aqueous stability were synthesized. SN1 and SN2 reduced the survival of human CRC HT-29 and HCT-116 cell lines, caused cell cycle arrest in G_2/M phase, and we observed downregulation of the expression of cyclin B1 and cyclin-dependent kinase 1 (Cdk1) along with up-regulation of the active form of p53, p21 and Bcl-2–associated X (Bax). Furthermore, SN1 and SN2 induced apoptosis by the intrinsic pathway, since they lead to the cleavage of caspase 9, caspase 3 and poly(ADP-ribose) polymerase (PARP), and up-regulating Bax. Phosphatidylinositol-3-kinase/protein kinase B (PI3K/Akt), nuclear factor-κB (NF-κB) and extracellular signal-regulated kinases (ERK) are important for cell survival and proliferation. SN1 and SN2 lead to decrease in the activity of Akt where the phosphorylated form decreased with time as well as they caused an important decrease in the phosphorylation of ERK and activity of NF-κB. Finally, SN1 and SN2 complexes affected p38/mitogen-activated protein kinase (MAPK) pathway then we recorded an increase in the cyclooxygenase-2 expression and its enzymatic product prostaglandin E_2.

1. Introduction

In the western world, colorectal cancer (CRC) is among the leading cause of cancer related death as it is the third most commonly diagnosed cancer in men and the second in women [1]. Lifestyle risk factors, principally nutritional practices, may play an important role in the development of CRC [2]. This development is a complex process involving multiple molecular pathways, from the formation of adenomas to the development of carcinoma in the digestive tract [3].

Chemotherapeutic colorectal agents are commonly used and usually given in the form of combinational chemotherapy. Cisplatin, which is one of the most widely used metal anticancer drugs, has been recognized as one of the most effective agents against colon cancer [4]. However, cisplatin induces drug resistance, and its side effects still are major limitations to its clinical use [5]. Among the non-platinum antitumor agents, gold complexes are receiving increasing attention because of their promising in vitro and in vivo anticancer activities [6,7]. A number of gold(III) complexes have been reported to exhibit cytotoxicity against abroad spectrum of tumor cells, and their potencies (IC_{50} values in low micromolar range) are comparable with that of cisplatin [8]. In recent years, a number of gold(III) complexes supported by strong donor ligands, such as porphyrins, have been reported to possess good stability and display potent anticancer activity [9]. Among them, gold(III) tetraphenyl-porphyrin chloride [Au(TPP)]Cl is stable under physiological conditions, resistant to reduction by glutathione, highly cytotoxic to various cancer cell lines, including cisplatin-resistant cancer cells and multidrug-resistant cells, and exhibits potent in vivo anticancer properties in multiple animal tumor models [10].

* Corresponding author at: LCSN, EA1069, Department of Biochemistry, Faculté de Pharmacie, Université de Limoges, 2 rue du Docteur Marcland, 87025 Limoges, France.
E-mail address: bertrand.liagre@unilim.fr (B. Liagre).

http://dx.doi.org/10.1016/j.jinorgbio.2017.08.024
Received 11 June 2017; Received in revised form 24 August 2017; Accepted 25 August 2017
Available online 06 September 2017
0162-0134/

Apoptosis, programmed cell death, is a common physiological process that is controlled by multiple genes and involves numerous biological events. Apoptosis involves two fundamental pathways: the extrinsic pathway, which transmits death signals by the death receptor, and the intrinsic pathway, which is initiated by intracellular stimuli [11]. Apoptosis and cell cycle are intimately coupled. The linkage of cell cycle and apoptosis has been recognized for some proteins such as: c-Myc, p53, pRb, cyclin-dependent kinase (CDK), cyclins and cyclin-dependent kinase inhibitor (CKI) [12]. Cell cycle is regulated by two major checkpoints at G1/S and G2/M transition. A defect in the regulation of any of these mechanisms often results in genomic instability, which predisposes the cell to malignant transformation [13].

Recent observations indicate that two of the most implicated cellular pathways in cancers are the phosphatidylinositol-3-kinase/protein kinase B (PI3K/Akt) and the mitogen-activated protein kinase (MAPK), the Raf-Ras-MEK-extracellular signal-regulated kinases (ERK) pathway, since they play a key role in the regulation of proliferation, differentiation and survival [14]. For instance, mutations affecting Ras, B-Raf, PI3K and Akt are common in perpetuating the malignancy of several types of cancers and increasing the resistance to apoptosis [12] [15].

A significant effort has been made to identify novel drug targets for CRC prevention and treatment. One group of compounds found to decrease the risk of CRC includes nonselective nonsteroidal anti-inflammatory drugs (NSAIDs), which target the cyclooxygenase enzymes (COX-1 and COX-2). Since elevated COX-2 expression was found in approximately 50% of adenomas and 85% of adenocarcinomas and is associated with worse survival among CRC patients [16], it was hypothesized that COX-2 contributes to chemoresistance in several cancers. Moreover, COX-2 and its enzymatic product prostaglandin E_2 (PGE_2) have key roles in influencing the development of CRC. Deregulation of the COX-2/PGE_2 pathway appears to affect colorectal tumorigenesis via a number of distinct mechanisms: promoting tumor maintenance and progression, encouraging metastatic spread, and perhaps even participating in tumor initiation [17].

In the present study, a novel gold(III) porphyrin analogues [gold(III) porphyrin-adamantane chloride (SN1) and gold(III) porphyrin-mono-acetate chloride (SN2)] (Fig. 1) were prepared by modifying one of the peripheral phenyl groups of ([Au(TPP)]Cl), to be a promising drug lead for anti- CRC treatment. This modification should improve its aqueous solubility and help in the construction of a delivery system for anticancer gold porphyrin complexes. Indeed, the presence of adamantane (hydrophobic guest molecule) will be used as host guest agent with β-cyclodextrin (βCD) (host molecule) which will be conjugated to the surface of nanoparticles (cellulose nanocrystals, …) to obtain a nanocarrier [18,19]. The acetyl group will be used to compare efficiency of this strategy of host-guest interaction. In connection with our research program on vectorization of hydrophobic molecules for an anticancer applications (RGD peptides, polyamines, iron oxide nanoparticles, mesoporous silica nanoparticles, etc.), this strategy is based on the increase of interest for nanoparticles aimed to passively target tumor tissues, thanks to the enhanced permeation and retention (EPR) effect [20,21]. This nanotechnology-based delivery systems should improve the internalization of nanovector/drug complexes, their biodistribution and decrease their toxicity while maintaining efficacy which is a key strategy to optimize and develop anticancer gold medicines [10]. Then, in order to release the gold porphyrin from β-cyclodextrin, the ester linkage, which was employed to conjugate the adamantane or acetyl and gold(III) porphyrin moiety, could be hydrolyzed readily by intracellular esterases or by acidic medium in the tumor microenvironment [22,23]. The efficacy of SN1 and SN2 on colon cancer cells was evaluated in vitro, and they showed an induction of cell cycle arrest and apoptosis, and inhibition of cell survival pathways.

2. Experimental

2.1. Materials and methods

All reagents, solvents and chemicals were purchased from Sigma-Aldrich Co, VWR, TCI or Alfa Aesar. The 5-(4-hydroxyphenyl)-10,15,20-tri(phenyl) porphyrin TPPOH was synthesized according to published procedure [24]. Ultraviolet (UV) spectra were recorded on a Specord 210 spectrophotometer (Analytik Jena) using 10-mm quartz cells. ^1H and ^{13}C NMR spectra were obtained on Brüker DPX-400 MHz spectrometer or on Brüker DPX-500 MHz spectrometer using tetramethylsilane as an internal reference. High-resolution mass spectra (HRMS) were acquired in positive mode with an ESI source on a Q-TOF mass spectrometer. (For ^1H NMR spectra, ^{13}C NMR spectra and HRMS

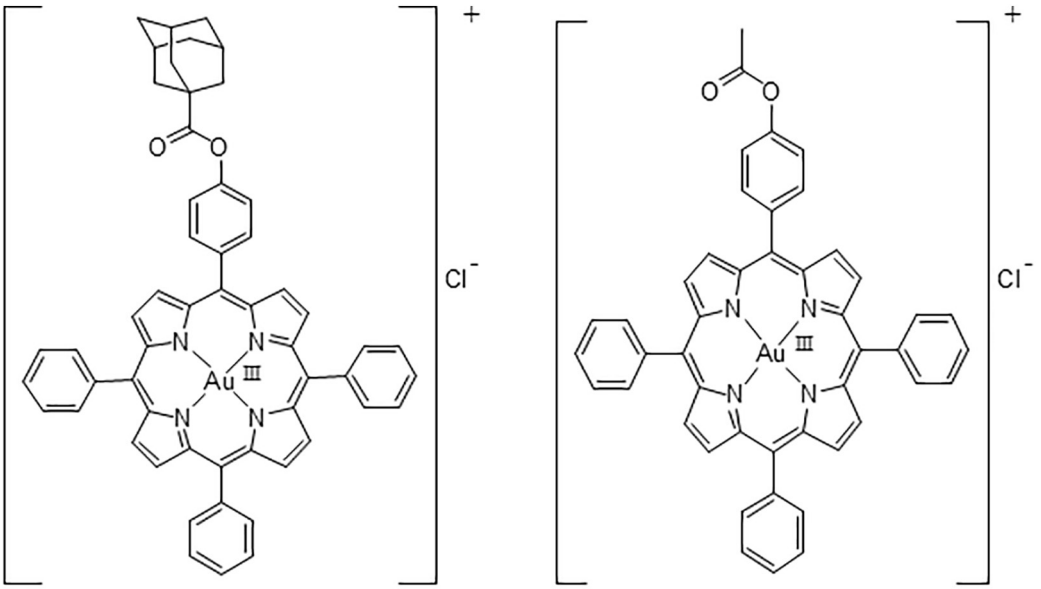

Gold(III) porphyrin-adamantane complex (SN1)

Gold(III) porphyrin-acetyl complex (SN2)

Fig. 1. Chemical structure of gold(III) porphyrin-adamantane chloride complex (SN1) and gold(III) porphyrin-mono-acetate chloride complex (SN2).

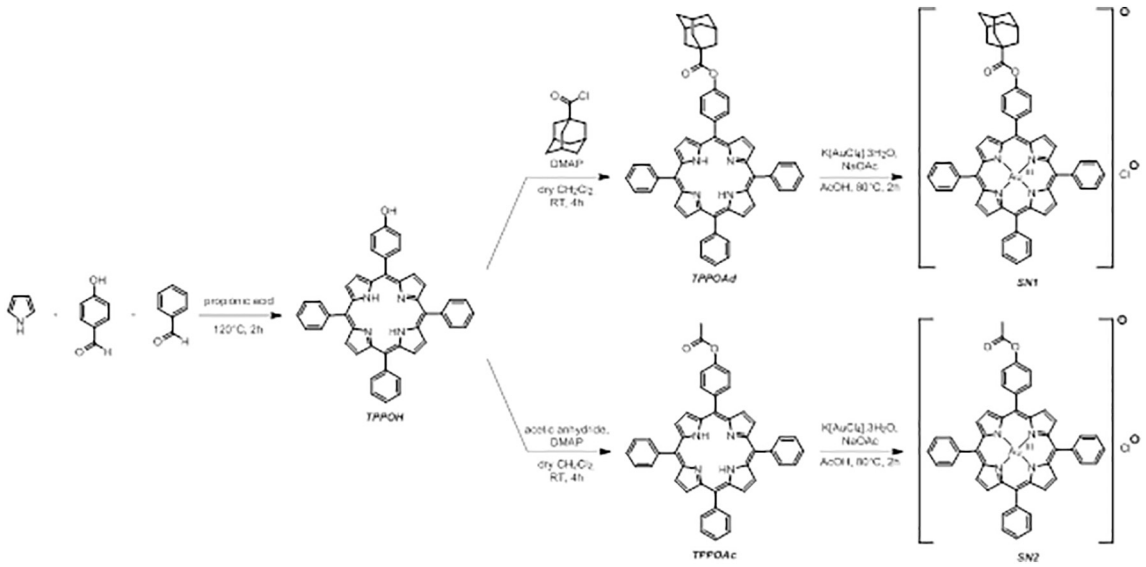

Scheme 1. Synthesis of gold(III) porphyrin complexes.

of 5-(4-(1-adamantanecarbonyloxy)phenyl)-10,15,20-triphenylporphyrin (TTPOAd), 5(4-acetoxyphenyl)[(10, 15, 20-triphenyl)porphyrin] (TTPOAc), SN1 and SN2, see supporting information: Fig. S1 to Fig. S10.)

2.2. Gold(III) porphyrin complexes synthesis (Scheme 1)

2.2.1. TPPOAd

A solution of 5-(4-hydroxyphenyl)-10,15,20-tris(phenyl) porphyrin (0.498 mmol), adamantane-1-carbonyl chloride (1.494 mmol), and DMAP (2.060 mmol) in dry CH_2Cl_2 (100 mL) was stirred at room temperature until all starting phenol -porphyrin was consumed (TLC, $CHCl_3$/petroleum ether (3:7, v/v), ~ 4 h). Solvents were evaporated, and the residue was purified by chromatography (SiO_2, $CHCl_3$/petroleum ether (3:7, v/v), upgrade $CHCl_3$/petroleum ether (4:6, v/v) and $CHCl_3$/petroleum ether (5:5, v/v)). The porphyrin was obtained as a purple solid in 75% yield (296.2 mg).

^{1}H NMR (500 MHz, $CDCl_3$): δ_H, (ppm) 8.84–8.87 (m, 8H, β-pyrrole-CH), 8.20–8.22 (m, 8H, o-Ph-CH and o-Ar-CH), 7.71–7.79 (m, 9H, m- and p-Ph-CH), 7.45 (d, 2H, J = 8.35 Hz, m-Ar-CH), 2.23 (bs, 6H, Adam-CH_2), 2.18 (bs, 3H, Adam-CH), 1.86 (bs, 6H, Adam-CH_2), − 2.77 (s, 2H, inner-NH). (Fig. S1).

^{13}C NMR (125.8 MHz, $CDCl_3$): δ 176.4 (1C, carbonyl-C), 151.0 (1C, Ar-CO), 142.2 (3C, Ph-C), 139.5 (1C, Ar-C), 135.3 (2C, o-Ar-CH), 134.6 (6C, o-Ph-CH), 131.1 (bs) (8C, β-pyrrole-CH), 127.7 (3C, p-Ph-CH), 126.7 (6C, m-Ph-CH), 120.24 (1C, *meso* C_{15}-C), 120.21 (2C, meso C_{10}- and C_{20}-C), 119.9 (2C, m-Ar-CH), 119.1 (1C, meso C_5-C), 41.3 (1C, Adam-C), 39.0 (3C, Adam-CH_2), 36.6 (3C, Adam-CH_2), 28.0 (3C, Adam-CH). Alpha carbons signals of free porphyrin are not observed (Fig. S2). UV-vis ($CHCl_3$), λ_{max} (nm) ($\varepsilon{\cdot}10^{-3}$ L·mmol^{-1}·cm^{-1}): 418 (618.5), 516 (23.5), 551 (12.0), 591 (8.6); 645 (6.4). HRMS(ESI): *m/z* calcd for $C_{55}H_{44}N_4O_2$ 792.963, $[M + H]^+$ found 793.354, $[M + 2H]^+$ 794.357 (Fig. S5).

2.2.2. SN1 (Fig. 1)

$K[AuCl_4]{\cdot}3H_2O$ (0.0584 mmol) and sodium acetate (0.253 mmol) were heated to 80 °C in acetic acid (10 mL) for 15 min. A solution of free porphyrin (0.0192 mmol) in acetic acid (10 mL) was added dropwise. The mixture was stirred and heated at 80 °C under argon. After 2 h, the solvent was evaporated to dryness and the residue was purified by preparative thin layer chromatography (TLC) (silica, $CHCl_3$/ethanol; 9/1). The expected compound was obtained as a brown-orange solid in 45% yield (12 mg). Rf = 0.9 ($CHCl_3$/ethanol: 95/5). ^{1}H NMR (400 MHz, $CDCl_3$) δ_H, (ppm) 9.25 (m, 8H, β-pyrrole-CH), 8.29 (m, 8H, o-Ph-CH and o-Ar-CH), 7.84 (m, 9H, m- and p-Ph-CH), 7.54 (d, J = 8.44, 2H, m-Ar-CH), 2.23 (s, 6H, Adam-CH_2), 2.21 (m, 3H, Adam-CH), 1.86 (s, 6H, Adam-CH_2) (Fig. S3). ^{13}C NMR (125 MHz, $CDCl_3$) δ (ppm) 176.4 (1C, carbonyl-C), 152.3 (1C, Ar-CO), 138.4 (3C, Ph-C), 137.0 (2C, α-pyrrole-C), 136.9 (6C, α-pyrrole-C), 135.6 (1C, Ar-C), 135.1 (2C, o-Ar-CH), 134.2 (6C, o-Ph-CH), 132.48 (2C, β-pyrrole-CH), 132.43 (4C, β-pyrrole-CH), 132.3 (2C, β-pyrrole-CH), 129.6 (3C, p-Ph-CH), 127.8 (6C, m-Ph-CH), 123.8 (1C, *meso* C_{15}-C), 123.7 (2C, meso C_{10}- and C_{20}-C), 122.7 (1C, meso C_5-C), 121.1 (2C, m-Ar-CH), 41.4 (1C, Adam-C), 38.9 (3C, Adam-CH_2), 36.5 (3C, Adam-CH_2), 28.0 (3C, Adam-CH) (Fig. S4). UV-vis ($CHCl_3$), λ_{max} (nm) ($\varepsilon{\cdot}10^{-3}$ L·mmol^{-1}·cm^{-1}) 410 (158.1), 523 (7.0). MS (7.0). MS (MALDI-TOF): *m/z* cald for $C_{55}H_{42}AuN_4O_2$ 987.2973, $[M]^+$ 987.2959 (Fig. S5).

2.2.3. TPPOAc

A solution of 5-(4-hydroxyphenyl)-10,15,20-tris(phenyl) porphyrin (300 mg, 0.475 mmol), acetic anhydride (135 μL, 1.426 mmol), and DMAP (87.1 mg, 0.713 mmol) in dry CH_2Cl_2 (30 mL) was stirred at room temperature until all starting phenol -porphyrin was consumed (TLC, $CHCl_3$/petroleum ether: 95/5, ~ 4 h). Solvents were evaporated, and the residue was purified by chromatography ($CHCl_3$/petroleum ether: 8/2, 9/1 and $CHCl_3$). The porphyrin was obtained as a purple solid in 70% yield (223.8 mg). Rf = 0.6 ($CHCl_3$/petroleum ether: 95/5). ^{1}H NMR (500 MHz, $CDCl_3$) δ_H, (ppm) 8.85 (m, 8H, β-pyrrole-CH), 8.21 (m, 8H, o-Ph-CH and o-Ar-CH), 7.74 (m, 9H, m- and p-Ph-CH), 7.48 (d, J = 8.48 Hz, 2H, m-Ar-CH), 2.48 (s, 3H, CH_3), − 2.78 (s, 2H, inner-NH) (Fig. S6). ^{13}C NMR (125.8 MHz, $CDCl_3$): δ 169.5 (1C, carbonyl-C), 150.6 (1C, Ar-CO), 142.1 (3C, Ph-C), 139.7 (1C, Ar-C), 135.3 (2C, o-Ar-CH), 134.6 (6C, o-Ph-CH), 132.3 (bs) (8C, β-pyrrole-CH), 127.7 (3C, p-Ph-CH), 126.7 (6C, m-Ph-CH), 120.3 (1C, *meso* C_{15}-C), 120.2 (2C, meso C_{10}- and C_{20}-C), 119.8 (2C, m-Ar-CH), 118.9 (1C, meso C_5-C), 21.4 (1C, CH_3). Alpha carbons signals of free porphyrin are not observed (Fig. S7). UV-vis ($CHCl_3$), λ_{max} (nm) ($\varepsilon{\cdot}10^{-3}$ L·mmol^{-1}·cm^{-1}) 418 (759.0), 516 (30.7), 550 (12.8), 591 (8.8), 646 (5.8). MS (MALDI-TOF): *m/z* calcd for $C_{46}H_{52}N_4O_2$ 672.771, $[M + H]^+$ found 673.2595 and $[M + 2H]^+$ 674.2627 (Fig. S10).

2.2.4. SN2 (Fig. 1)

$K[AuCl_4]{\cdot}3H_2O$ (1.78 mmol) and sodium acetate (5.945 mmol) were heated to 80 °C in acetic acid (10 mL) for 15 min. A solution of TPPOAc (0.0192 mmol) in acetic acid (10 mL) was added dropwise. The mixture was stirred and heated at 80 °C under argon for 2 h. The solvent was

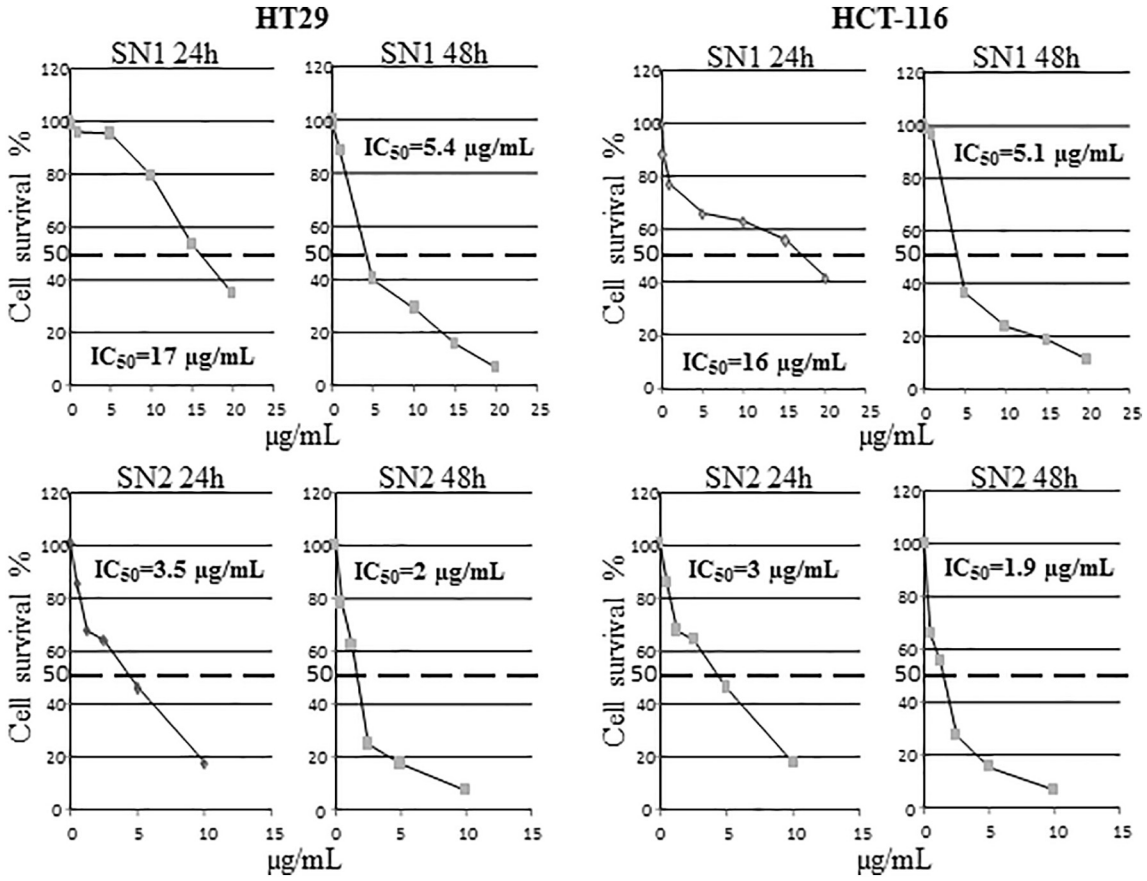

Fig. 2. Effect of SN1 or SN2 on cell proliferation. HT-29 and HCT-116 cells were treated at indicated concentrations and relative cell viability was assessed by MTT dye exclusion method for 24 and 48 h. Results were expressed as percentage of cell survival compared to control, and IC_{50} was determined for each condition. Results were expressed as means ± SD of three independent experiments.

Table 1
IC_{50} values of SN1 and SN2 on human colorectal cancer cells.

	HT-29 cells		HCT-116 cells	
	24 h	48 h	24 h	48 h
SN1 (IC_{50} µg/mL)	17	5.4	16	5.1
SN2 (IC_{50} µg/mL)	3.5	2.0	3.0	1.9

evaporated to dryness and the residue was purified by preparative TLC (silica, $CHCl_3$/ethanol; 9/1). The expected compound was obtained as a brown-orange solid in 56% yield (30 mg). Rf = 0.7 ($CHCl_3$/ethanol:9/1). ^{1}H NMR (400 MHz, $CDCl_3$) δ_H, (ppm) 9.26 (m, 8H, β-pyrrole-CH), 8.30 (m, 8H, o-Ph-CH and o-Ar-CH), 7.84 (m, 9H, m- and p-Ph-CH), 7.75 (d, J = 8.44, 2H, m-Ar-CH), 2.50 (s, 3H, CH_3) (Fig. S8). ^{13}C NMR (125 MHz, $CDCl_3$) δ (ppm) 169.4 (1C, carbonyl-C), 151.7 (1C, Ar-CO), 138.9 (3C, Ph-C), 137.06 (2C, α-pyrrole-C), 137.05 (2C, α-pyrrole-C), 137.01 (4C, α-pyrrole-C), 136.4 (1C, Ar-C), 135.3 (2C, o-Ar-CH), 134.4 (6C, o-Ph-CH), 132.3 (2C, β-pyrrole-CH), 132.2 (4C, β-pyrrole-CH), 132.1 (2C, β-pyrrole-CH), 129.3 (3C, p-Ph-CH), 127.6 (6C, m-Ph-CH), 123.7 (3C, *meso* C_{10}-, C_{15}- and C_{20}-C), 122.5 (1C, meso C_5-C), 120.8 (2C, m-Ar-CH), 21.4 (1C, CH_3) (Fig. S9). UV–vis ($CHCl_3$), λ_{max} (nm) ($\varepsilon.10–^3$ L·mmol^{-1}·cm^{-1}) 411 (293.5), 523 (15.0). MS (MALDI-TOF): *m/z* calcd for $C_{46}H_{30}AuN_4O_2$ 867.203, $[M]^+$ 867.203 and [M + H] + 868.203 (Fig. S10).

2.3. Cell lines, cell culture, and treatment

Human colorectal cell lines HT-29 and HCT-116 were purchased from American Culture Type Collection (LGC Standards, Middlesex, UK). HT-29 and HCT-116 cells were grown, respectively in DMEM and RPMI-1640 (Gibco BRL, Cergy-Pontoise, France) supplemented with 10% fetal calf serum (FCS) (Gibco BRL), 100 U/mL penicillin and 100 µg/mL streptomycin (Gibco BRL). Cultures were maintained in a humidified atmosphere with 5% CO_2 at 37 °C. For all experiments, cells were seeded at 3×10^4 cells/cm^2 for HT-29 and HCT-116 cells and were grown for 24 h in culture medium prior to exposure or not to SN1 or SN2 at indicated concentration. A 5 mg/mL and 1.806 mg/mL for SN1 and SN2 respectively stock solutions were prepared in dimethyl sulfoxide (DMSO), and diluted in culture medium to give the appropriate final concentrations. The same amount of vehicle (percentage of DMSO did not exceed 0.55%) was added to control cells. For other conditions, HT-29 cells were pre-treated for 2 h with 10 µM NS-398 (COX-2 inhibitor; Cayman Chemical, Bertin Pharma, Montigny le Bretonneux, France) before adding SN1 or SN2 for 24 and 48 h.

2.4. Cell proliferation assay

Measurement of cell proliferation was determined using the 3-(4,5-dimethylthiazol-2-yl)-2,5-diphenyltetrazolium bromide (MTT) assay. HT-29 and HCT-116 cells were grown for 24 h then treated with SN1 or SN2 at indicated concentrations. MTT tests were carried out daily as previously described [25] and experiments were performed in three independent assays.

2.5. Cell cycle analysis by flow cytometry (FACS)

The HT-29 and HCT-116 cells were seeded, grown for 24 h and then treated or not with the SN1 or SN2 for 24 and 48 h. For flow cytometry, 2×10^6 cells were washed with phosphate buffered saline (PBS), and

A

24 h	G0-G1	S	G2-M	Sub-G1
Control	45.99	23.53	24.19	0.84
SN1 16 µg/mL	52.11	11.19	34.39	2.74

24 h	G0-G1	S	G2-M	Sub-G1
Control	44.40	26.90	28.10	0.50
SN2 3 µg/mL	48.70	14.50	34.90	2.20

48 h	G0-G1	S	G2-M	Sub-G1
Control	56.72	20.72	12.36	0.87
SN1 16 µg/mL	51.40	16.61	23.40	9.74

48 h	G0-G1	S	G2-M	Sub-G1
Control	62.00	19.00	18.30	0.80
SN2 3 µg/mL	45.20	13.40	30.20	10.30

B

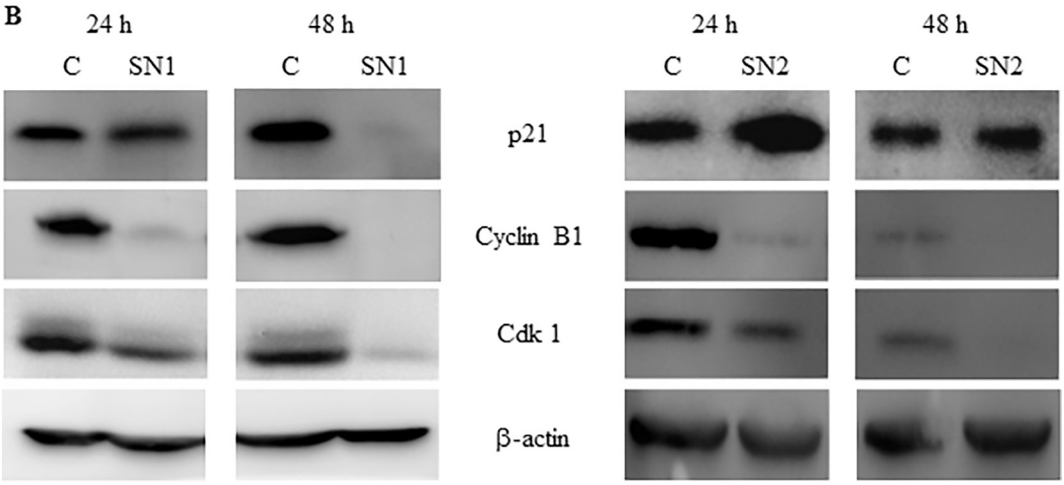

Fig. 3. Effect of SN1 or SN2 on cell cycle distribution and its regulators in HCT-116 cells. **(A)** Results of flow cytometric analysis are represented by percentage of cells in each cell cycle phase. **(B)** Protein expression in whole cell lysates was measured by Western Blot. β-Actin was used as an internal control. Blots are representative of three separate experiments.

fixed with 1 mL of chilled 70% ethanol in PBS at − 20 °C. Following fixation, cells were pelleted, washed twice in cold PBS, resuspended in 500 mL of cold PBS and 30 µL ribonuclease A (RNase A) (10 mg/mL; Roche Diagnostics, Meylan, France), and incubated for 30 min at room temperature. After staining with 25 µL propidium iodide (1 mg/mL; Invitrogen Life Technologies, Saint-Aubin, France), the percentage of cells in each stage of the cell cycle was determined using FACS system (BD Biosciences, San Jose, CA).

2.6. Protein extraction and Western Blot analysis

For total protein extraction, HT-29 and HCT-116 cells were washed in PBS, then, the total cell pool (attached and floating cells) was centrifuged at 200 g for 5 min at 4 °C and homogenized in RIPA lysis buffer (50 mM HEPES, pH 7.5, 150 mM NaCl, 1% sodium deoxycholate, 1% NP-40, 0.1% SDS, 20 mg/mL of aprotinin) containing protease inhibitors (Complete™ Mini, Roche Diagnostics) according to the manufacturer's instructions. Proteins (10–100 µg) were separated by electrophoresis on 10% SDS–PAGE gels and transferred to polyvinylidene fluoride (PVDF) membranes (Amersham Pharmacia Biotech, Saclay, France) and probed with human primary antibodies. Human antibody against Cdk1, caspase-9, caspase-3, cleaved caspase-3 and PARP-1 were purchased from Cell Signaling Technology (Ozyme, France), p21waf1/cip1, cyclin B1, p-p53 (Ser 15), p53, Bcl-2–associated X (Bax), Bcl-2, Akt, phospho-Akt (Ser 473) were purchased from Santa-Cruz Biotechnology (CliniSciences, Nanterre, France). COX-2 and β-actin antibodies were respectively purchased from Cayman Chemical (Bertin Pharma, Montigny le Bretonneux, France) and Sigma Aldrich (Saint Quentin Fallavier, France). After incubation with secondary antibodies (Dako France S.A.S., Trappes, France and Cell Signaling Technology, Ozyme, France), blots were developed using the ECL Plus Western Blotting Detection System (Amersham Pharmacia Biotech) and G: BOX system (Syngene, Ozyme, Saint Quentin en Yvelines, France). Membranes were then reblotted with anti-β-actin (Sigma Aldrich, Saint Quentin Fallavier, France) used as a loading control.

2.7. Apoptosis quantification: DNA fragmentation

HT-29 and HCT-116 cells were cultured in 75 cm^2 tissue culture flasks and allowed to grow for 24 h in culture medium prior exposure to treatment. HT-29 and HCT-116 cells were incubated alone or with SN1 or SN2 used at the respective IC_{50} for 24 and 48 h. The same concentrations were used for experiment with pretreatment of 10 µM NS-398 for 2 h. Apoptosis was quantified in the total cell pool (attached and floating cells) using the cell death enzyme-linked immunosorbent assay (ELISA) kit (Cell Death Detection ELISA plus, Roche Diagnostics). Cytosol extracts were obtained according to the manufacturer's protocol and apoptosis was measured as previously described [26].

2.8. Quantification of phospho-ERK1/2 and phospho-p38

After treatment, 10^6 cells were homogenized in a lysis buffer containing protease and phosphatase inhibitors in accordance with the manufacturer's protocol (R & D Systems, Lille, France). Phospho-ERK1/2 and phospho-p38 detection was performed according to the manufacturer's instructions (R & D Systems) as previously described [27].

2.9. Nuclear factor-κB (NF-κB) translocation

Subcellular protein fractionation – 12, 24 and 48 h after treatment, cells were recovered and cytosolic and nuclear fractions were obtained using the Subcellular Protein Fractionation Kit according to the manufacturer's protocol (Thermo Fischer Scientific, Rockford, IL, USA) as previously described [26]. Protein levels were determined using the

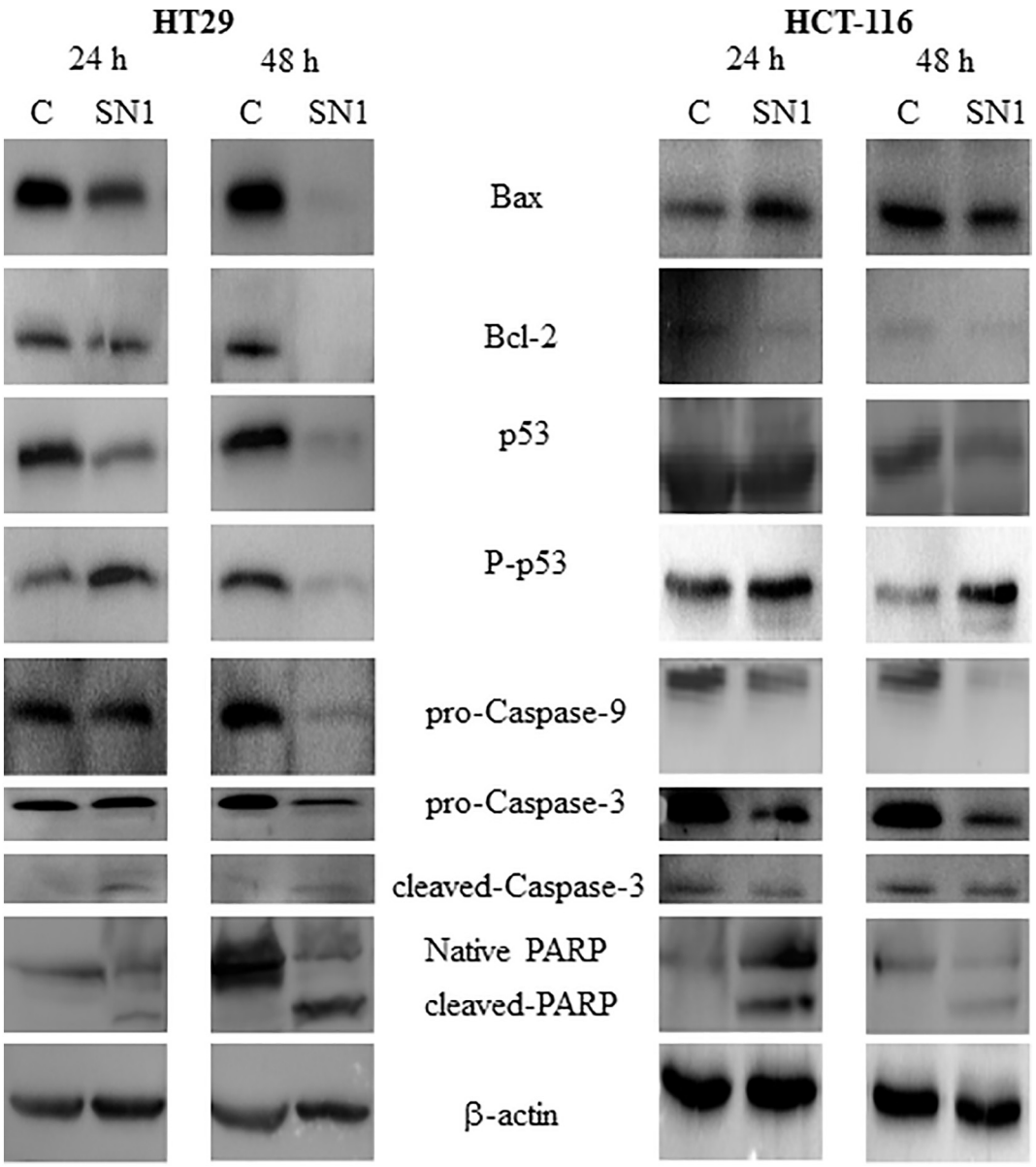

Fig. 4. Effect of SN1 on intrinsic apoptotic pathway in HT-29 and HCT-116 cells. HT-29 cells were treated with or without 17 or 5.4 μg/mL while HCT-116 cells were treated with or without 16 or 5.1 μg/mL SN1 for 24 and 48 h respectively. Protein expression in whole cell lysates was measured by Western Blot. β-Actin was used as an internal control. Blots are representative of three separate experiments.

Bradford method.

Electromobility shift assay (*EMSA*) – EMSA experiments were performed using digoxigenin (DIG) Gel Shift kit (Roche Diagnostics). Briefly, nuclear extracts were prepared from HT-29 and HCT-116 cells and NF-κB binding reactions were carried out with 10 μg nuclear proteins incubated with DIG labeled NF-κB probe according to the manufacturer's protocol, as previously described [28].

2.10. PGE_2 immunoassay

PGE_2 levels in culture medium were quantified in supernatants from treated or control HT-29 cells by enzyme immunoassay according to the manufacturer's instructions (PGE_2 EIA Kit, Cayman Chemical) as previously described [29,30].

2.11. Statistical analysis

Data are expressed as the arithmetic means ± standard deviation (SD) of separate experiments. The statistical significance of results obtained from in vitro studies was evaluated by the two tailed unpaired Student's *t*-test, with $p < 0.05$ being considered as significant.

3. Results

3.1. Synthesis of gold(III) porphyrin complexes SN1 and SN2 and study of their stability

Gold(III) porphyrin complexes SN1 and SN2 were prepared by the synthetic route shown in Scheme 1. The 5-(4-hydroxyphenyl)-10,15,20-tris(phenyl) porphyrin TPPOH was synthesized in 2.7% yield by treating freshly distilled pyrrole with benzaldehyde and 4-hydroxybenzaldehyde in propionic acid utilizing the reported method [24]. The two porphyrins TPPOAd and TPPOAc were obtained by esterification reaction between TPPOH and respectively adamantane-1-carbonyl chloride and acetic anhydride in presence of DMAP as catalyst. Gold(III) porphyrin compounds were synthesized by the treatment of K

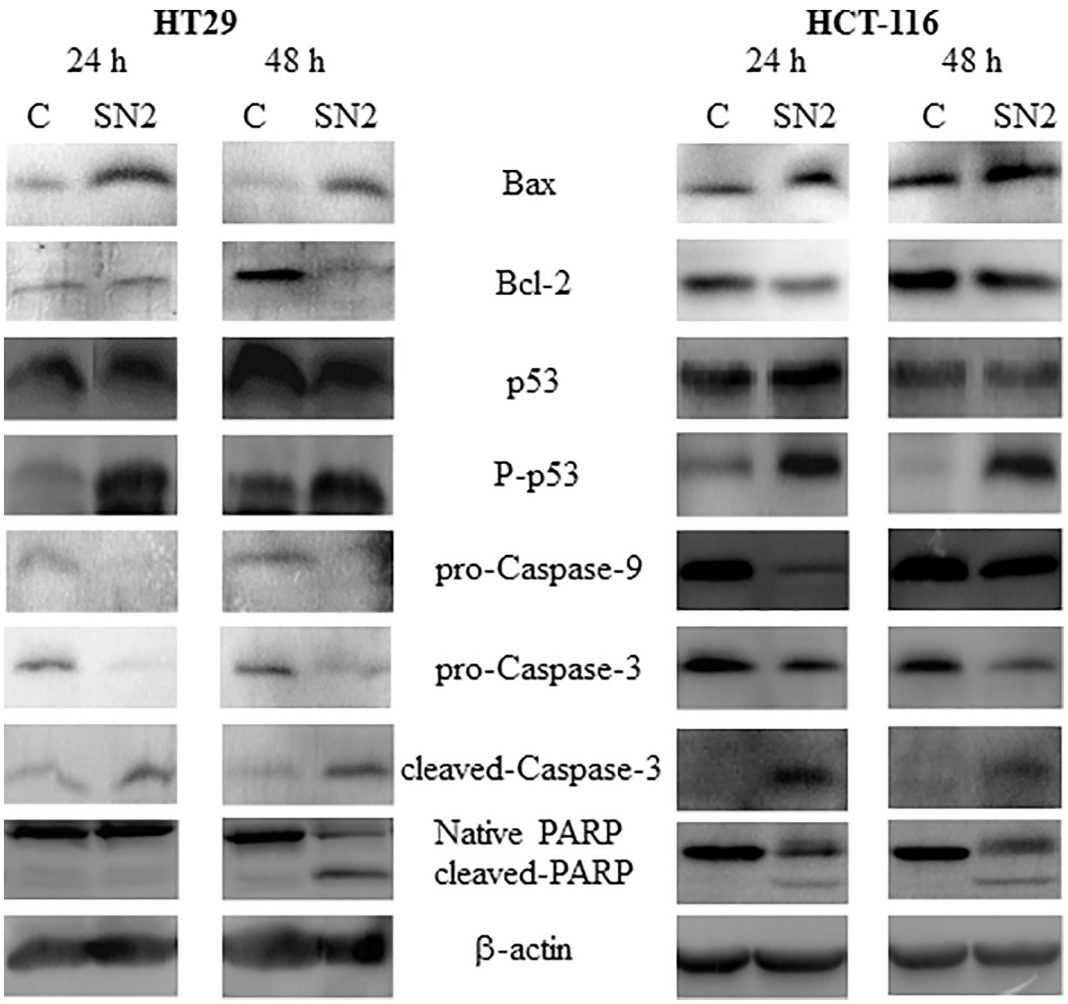

Fig. 5. Effect of SN2 on intrinsic apoptotic pathway in HT-29 and HCT-116 cells. HT-29 cells were treated with or without 3.5 or 2 μg/mL while HCT-116 cells were treated with or without 3 or 1.9 μg/mL SN2 for 24 and 48 h respectively. Protein expression in whole cell lysates was measured by Western Blot. β-Actin was used as an internal control. Blots are representative of three separate experiments.

$[Au^{III}Cl_4]$ with the free-base porphyrin ligand in the presence of NaOAc in acetic acid [31–33]. After purification with preparative thin layer chromatography, gold(III) porphyrin complexes SN1 and SN2 are obtained as chloride salts in 45 and 56% yields respectively. ^{1}H NMR, ^{13}C NMR, electrospray ionization (ESI) and UV–Vis spectroscopy were used to characterize the both compounds. In order to study the stability of gold(III) porphyrins SN1 and SN2, UV–visible spectra have been realized. The two compounds exhibit excellent stability in a PBS/acetone (1/1) solution, and no spectral changes were observed over 48 h at room temperature (Fig. S11).

3.2. SN1 and SN2 exhibited antiproliferative effect on CRC cells

After exposure to various concentrations of SN1 and SN2 for 24 and 48 h, the survival of colon cancer cells was assessed by MTT test. The inhibitory concentrations (concentration of the drug required to inhibit cell growth by 50% compared with control [IC_{50} values]) were evaluated from the dose dependence of cell surviving (Fig. 2). Results revealed that SN2 was more potent than SN1 (Table 1). SN1 has antiproliferative effect on HT-29 cells with IC50 at 24 h = 17 μg/mL and at 48 h = 5.4 μg/mL while on HCT-116 cells the IC_{50} at 24 h = 16 μg/mL and at 48 h = 5.1 μg/mL. SN2 demonstrated significant antiproliferative effect on HT-29 cells with IC_{50} at 24 h = 3.5 μg/mL and at 48 h = 2 μg/mL and on HCT-116 cells with IC_{50} at 24 h = 3 μg/mL and at 48 h = 1.9 μg/mL.

3.3. SN1 and SN2 caused cell cycle arrest in G2/M phase in HCT-116 cells but not in HT-29 cells

When HCT-116 cells were treated with the IC_{50} for SN1 and SN2 for 24 and 48 h, the percentage of cells in G2/M phase increased (at 24 h: 34.39% and 34.90% for SN1 and SN2, respectively vs. 24.19% and 28.10% for control; at 48 h: 23.40% and 30.20% for SN1 and SN2 respectively vs. 12.36% and 18.30% for control). Furthermore, a significant increase in the number of apoptotic cells was shown (sub-G1 cells, at 24 h: 2.74% and 2.20% for SN1 and SN2 respectively vs. 0.84% and 0.5% for control; at 48 h: 9.74% and 10.30% for SN1 and SN2 respectively vs. 0.87% and 0.8% for control) (Fig. 3A). No cell cycle arrest was observed for cells HT-29 (data not shown).

In separate experiments, SN1 and SN2-treated HCT-116 cells were lysed and proteins were extracted for Western Blotting. Consistent with the findings from cell cycle assay, time-dependent down-regulation of the expression of both G2/M regulatory proteins cyclin B1 and Cdk1 and increase of the expression of p21 protein especially after 24 h-treatment which is associated with linking DNA damage to cell cycle arrest were observed. These data indicated that SN1 and SN2 induce cell cycle arrest, resulting in the inhibition of cancer cell growth (Fig. 3B).

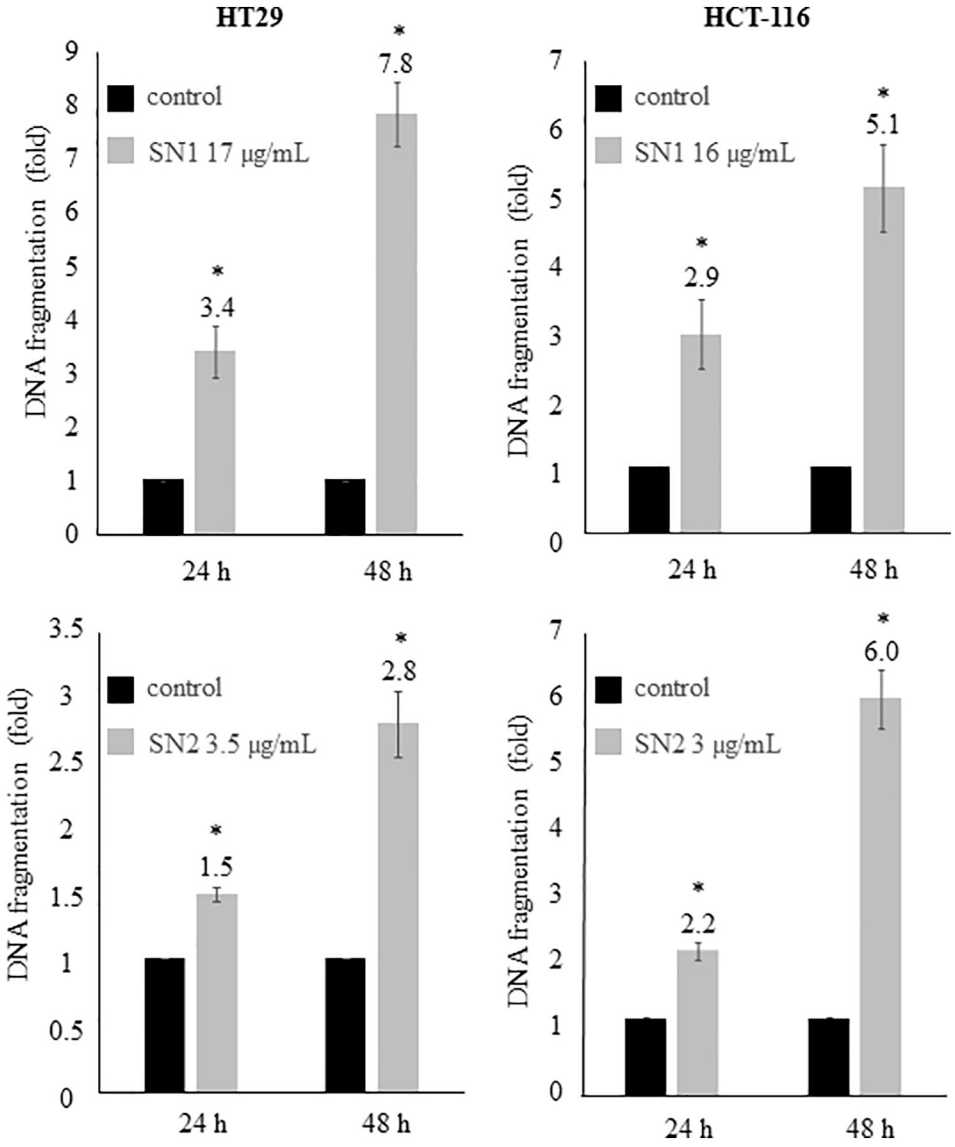

Fig. 6. SN1 or SN2 induced DNA fragmentation in HT-29 and HCT-116 cells. DNA fragmentation was quantified from cytosol extracts according to the manufacturer's instructions (Cell Death Detection ELISA plus, Roche Diagnostics). Results were reported as n-fold compared to controls. Values are expressed as mean ± SD ($p < 0.05$: *p-value relative to control group).

3.4. SN1 and SN2 induced apoptosis and DNA damage in CRC cells

To investigate the mechanism(s) of tumor death, HT-29 and HCT-116 cells were treated with SN1 and SN2 and markers of cellular apoptosis were assessed by Western Blot analysis. The analysis showed activation of caspase-9 by decreasing the expression of pro-caspase-9 in both cell lines which indicated that SN1 and SN2 activated the intrinsic death pathway (Figs. 4 and 5). In addition, treatment with SN1 and SN2 consistently resulted in the expression of several markers of apoptosis, such as cleaved-caspase-3, and PARP cleavage. Moreover SN1 and SN2 up-regulated the expression of p-p53 except at 48 h in HT-29 cells. Treatment with SN1 except in HT-29 cells and SN2 up-regulated the expression of Bax especially for SN2 and decreased the expression of Bcl-2 (Figs. 4 and 5).

Treatment with SN1 and SN2 induced marked morphologic changes, and increase DNA fragmentation in both cell lines. SN1 induced DNA fragmentation in HT-29 cells (+ 3.4 fold at 24 h and + 7.8 fold at 48 h for 17 µg/mL of SN1 versus control) as in the HCT-116 cells (+ 2.9 fold at 24 h and + 5.1 fold at 48 h for 16 µg/mL of SN1 versus control) (Fig. 6). Treatment with SN2 also induced DNA fragmentation in HT-29 cells (+ 1.5 at 24 h and + 2.8 fold at 48 h for 3 µg/mL of SN2 versus control) as in HCT-116 cells (+ 2.2 fold at 24 h and + 6.0 fold at 48 h for 3 µg/mL of SN2 versus control) (Fig. 6). Overall, these results confirmed the proapoptotic activity of SN1 and SN2 in HT-29 and HCT-116 cells.

3.5. Effect of SN1 and SN2 on PI3K/Akt, ERK1/2 and NF-κB survival pathways, and on p38 pro-apoptotic pathway

Resistance is a significant limitation to the effectiveness of cancer therapies. The PI3K/Akt and ERK1/2 pathways play important roles in a variety of normal cellular processes and tumorigenesis. Thus, PI3K/Akt and ERK1/2 pathways were investigated to show the anticancer effects of SN1 and SN2. We showed that both SN1 and SN2 decreased the expression of p-Akt, thus deactivation the PI3K/Akt pathway, from 12 h of treatment (Fig. 7). In addition, we found that SN1 and SN2 target the ERK1/2 pathway through dephosphorylation of ERK when HT-29 and HCT-116 cells were treated at different time intervals (Fig. 8A). On the contrary, Fig. 8B showed that SN1 and SN2 both induced p38 phosphorylation especially at 24 h- and 48 h-treatment.

Since NF-κB may be a critical regulator of cell survival and death and plays a critical role in apoptosis resistance, we studied the effect of SN1 and SN2 on nuclear activation of NF-κB. Results clearly showed that SN1 and SN2 inhibited NF-κB activation especially at 48 h for SN1 but more rapidly for SN2 from 12 h-treatment (Fig. 9). These findings indicate that SN1 and SN2 renders HT-29 and HCT1-116 colon cancer

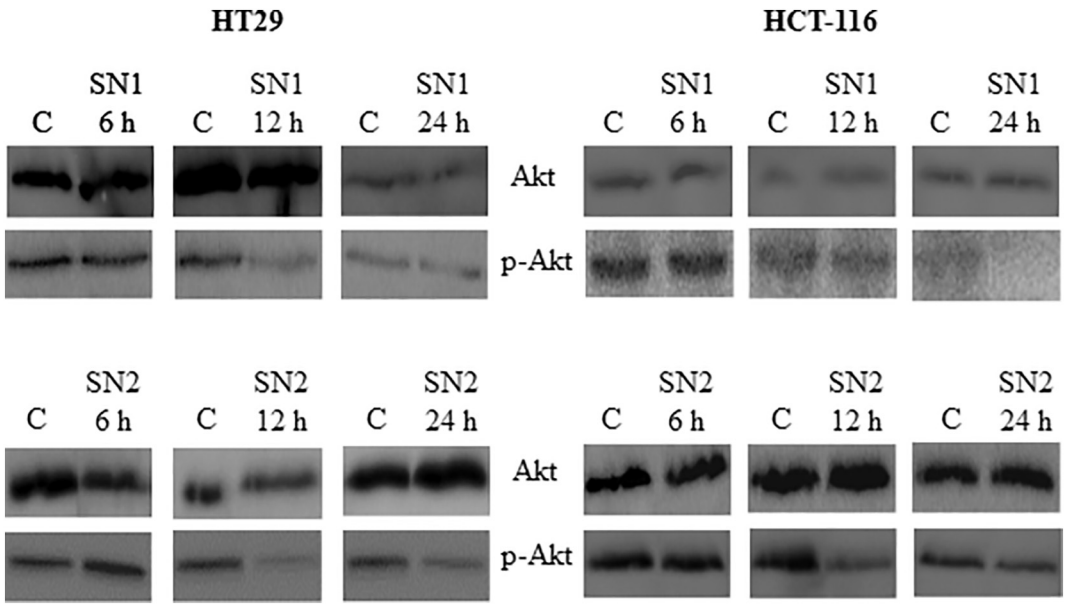

Fig. 7. Effects of SN1 or SN2 on Akt pathway known to be involved in apoptosis resistance in CRC cells. HT-29 cells were treated with or without 17 or 3.5 μg/mL while HCT-116 cells were treated with or without 16 or 3 μg/mL SN1 or SN2 respectively. After 6, 12 and 24 h, Akt and p-Akt expression were determined by Western Blot. Blots are representative of two separate experiments.

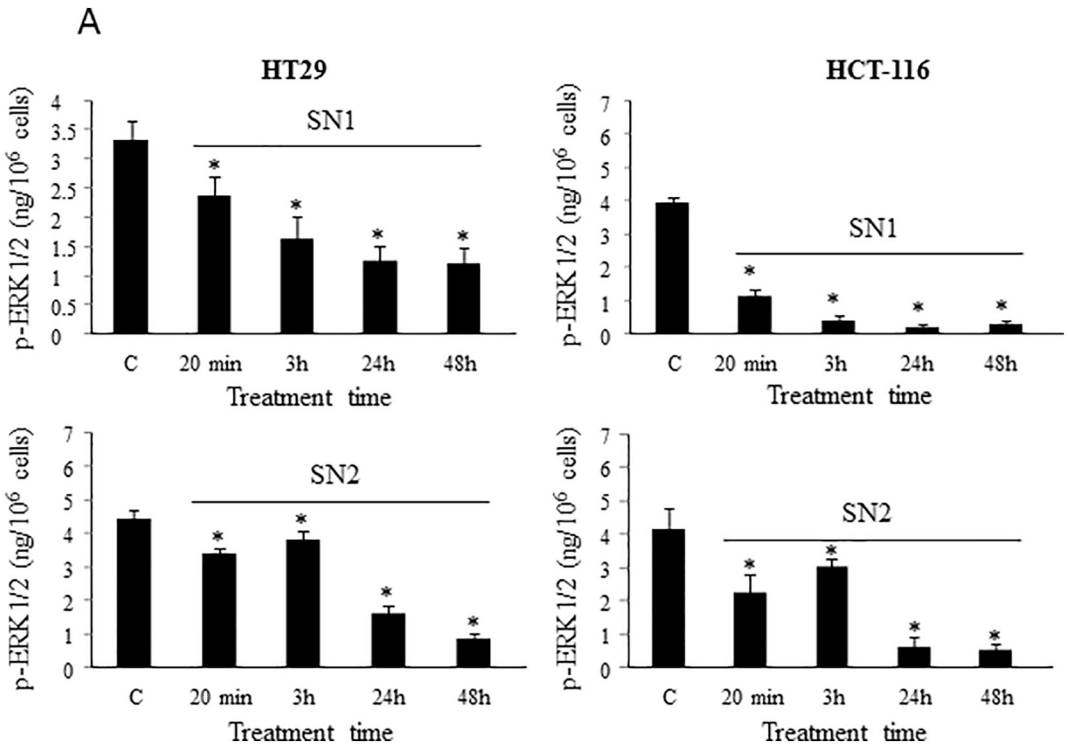

Fig. 8. Effects of SN1 or SN2 on ERK1/2 (A) and p38 (B) activation. HT-29 cells were treated with or without 17 or 3.5 μg/mL while HCT-116 cells were treated with or without 16 or 3 μg/mL SN1 or SN2 respectively. After indicated times, ERK1/2 and p38 phosphorylation were quantified with the Duo Sets IC assay kits (R & D Systems). Each value represents the mean ± SD from three separate experiments (*p*-value relative to control group, $*p < 0.05$).

cells more sensitive to apoptosis and could indeed be an effective treatment for drug resistant cells since they inhibit PI3K/Akt, ERK1/2 and NF-κB pathways.

3.6. SN1 and SN2 regulated p38/COX-2/PGE_2 pathway and effect of COX inhibition on inducing apoptosis

The elevated COX-2 expression was found in most CRC tissue and is associated with worse survival among CRC patients, so we were interested in studying the COX-2 expression and PGE_2 production. Because HCT-116 cells were COX-2 deficient, only HT-29 cells were treated with SN1 and SN2 and COX-2 expression was visualized by Western Blot and its activity by PGE_2 EIA assay. Results showed that SN1 and SN2 increased the expression (Fig. 10A) and activity (Fig. 10B) of COX-2 at 24 and 48 h. Furthermore, to confirm the role of COX-2 in apoptosis resistance, we showed that HT-29 has higher DNA fragmentation folds when treated with SN1 and SN2 combined with NS-398 (COX-2 specific inhibitor) at 24 h (+ 4.3 fold for NS-398 + SN1 vs. + 2

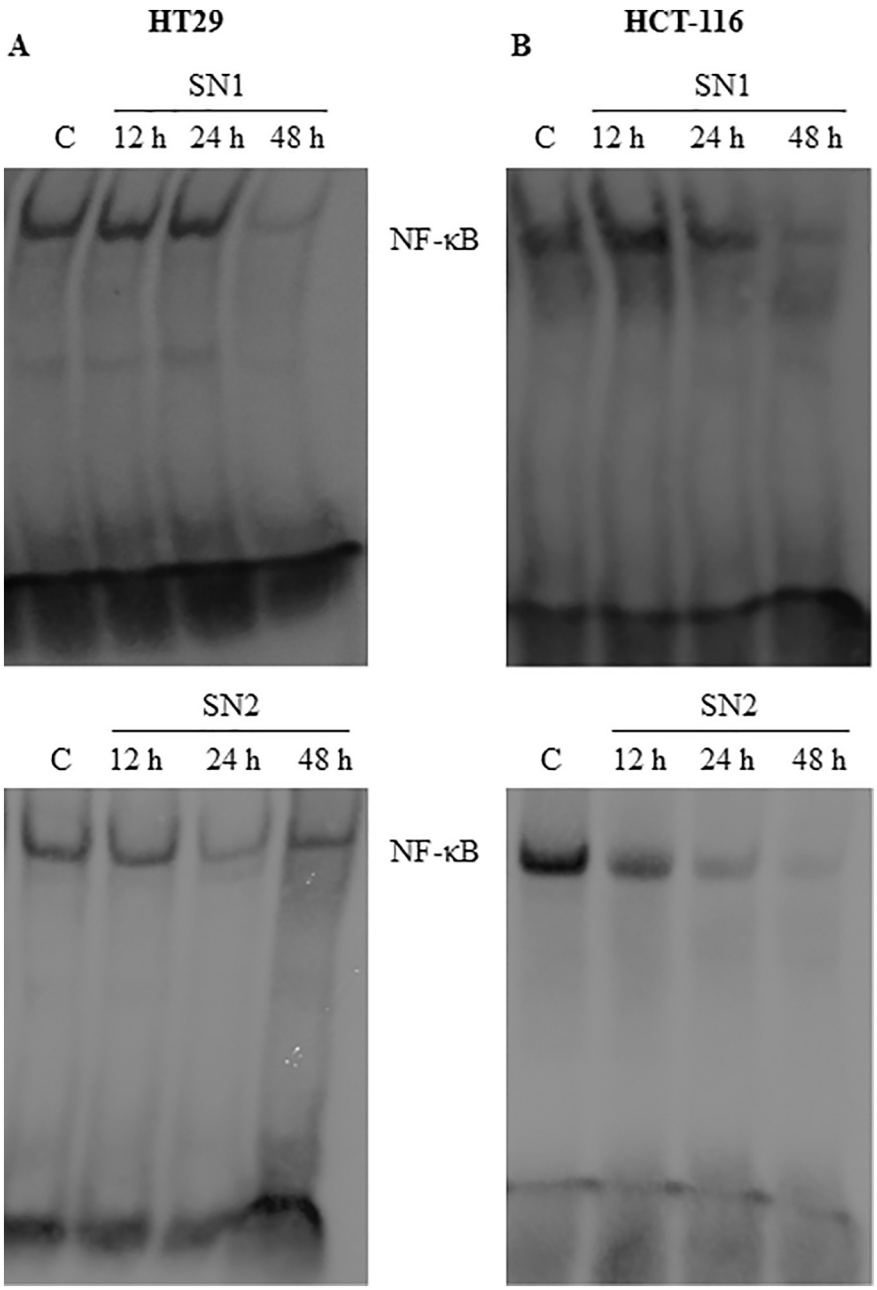

Fig. 9. Effect of SN1 or SN2 on NF-κB activation in HT-29 (A) and HCT-116 (B) cells. HT-29 cells were treated with or without 17 or 3.5 μg/mL while HCT-116 cells were treated with or without 16 or 3 μg/mL SN1 or SN2 respectively. After 12, 24 and 48 h, EMSA experiments were performed using DIG Gel Shift Kit (Roche Diagnostics) on nuclear extracts. Blots are representative of two separate experiments.

fold for SN1 alone and + 2.7 fold for NS-398 + SN2 vs. 1.9 fold for SN2 alone) (Fig. 10C).

4. Discussion

It has attracted much attention in recent years to find ways to increase specificity and selectivity of chemotherapy in cancer cells. Recent scientific articles show that complexes of ruthenium, iridium and platinum are the new metal-based drugs used in the treatment of several cancers such colon [34,35]. Gold and in particular gold(I), which is soluble in aqueous medium, is known to exhibit anticancer activities. Unfortunately, gold(I) complexes exhibited severe cardiotoxicity in animals. In contrast, gold(III), which is not stable in buffer solution (easily undergo decomposition to gold(I) and gold colloidal), can be used to prepare gold(III) porphyrin complexes. Indeed, the macrocycle ring made a rigid ligand scaffold, stabilize gold(III) complexes and avoid the decomposition to gold(I) [36]. Since most of the currently available chemotherapeutic agents are lacking ability to selectively target cancer cells, it is not surprising that interests for gold (III) porphyrin complexes as a potential anti-cancer drug have dramatically increased due to its enhanced selectivity and apoptosis inducing efficacy. We have studied the antitumor effect of two gold(III) porphyrin complexes: SN1 and SN2, and based on MTT test, they indeed significantly reduced the survival of human CRC HT-29 and HCT-116 cell lines with a more potent antiproliferative effect on HCT-116 (COX-2 deficient) than HT-29 (COX-2 sufficient) cells.

Gold(III) complexes exert their antiproliferative activities through mechanisms that are substantially different from those of platinum drugs [37]. Yet, the molecular mechanisms and targets of gold(III) porphyrin complexes remain uncharacterized. Some studies mention that the mitochondrial chaperone (Hsp60) is a direct molecular target of gold(III) porphyrins [38], also it is believed generally that the cytotoxic effects of metal complexes are the consequences of direct damage to nuclear DNA [4]. However, recent data indicated that the induction of apoptosis is a major mechanism of gold(III) porphyrin complexes [39–41]. Apoptosis is mediated by two central pathways, an

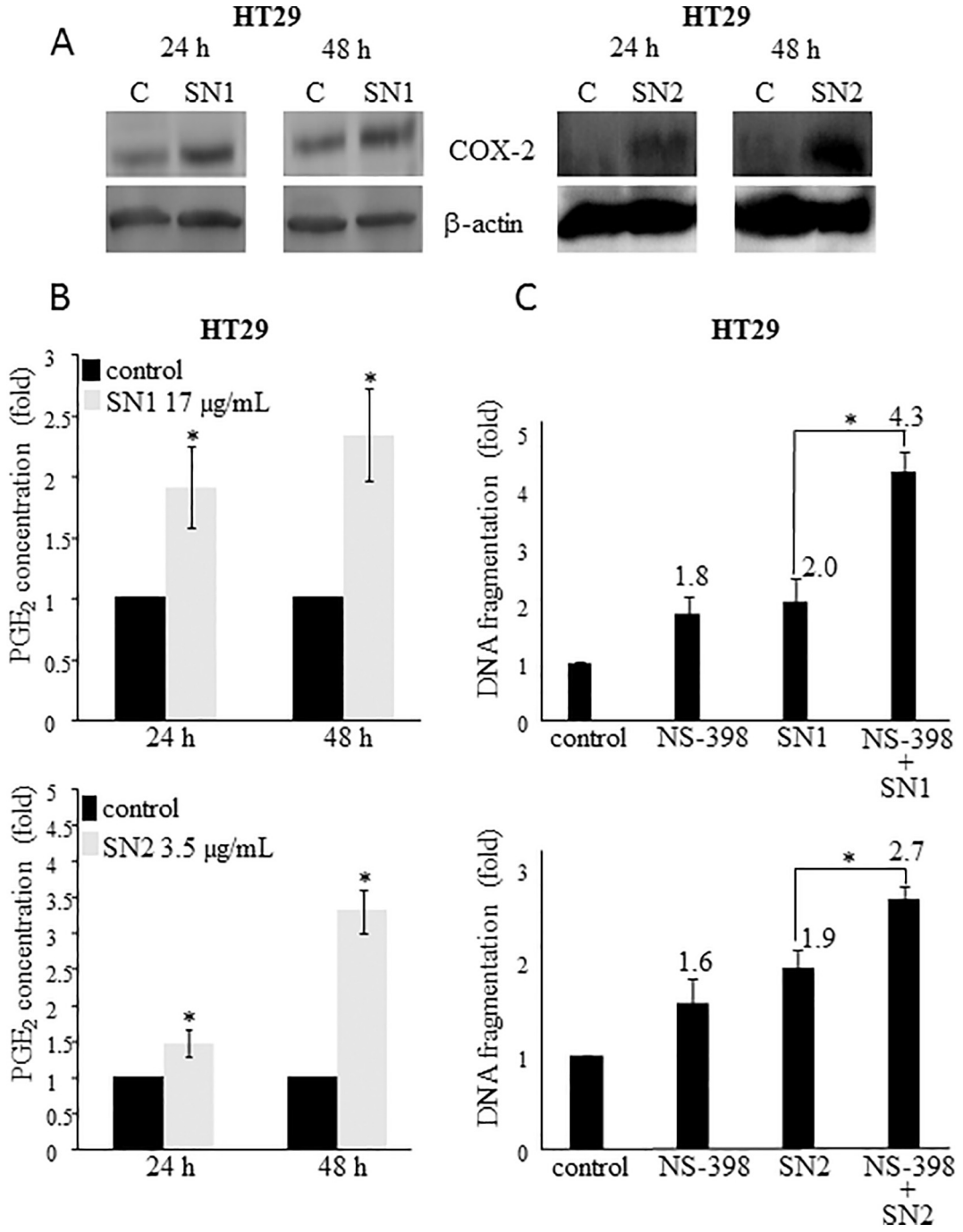

Fig. 10. COX-2 expression and activity in SN1- or SN2-treated cells, and effects of COX-2 inhibition on DNA fragmentation. (A) COX-2 expression was evaluated in the total cellular pool using Western blot analysis (β-actin was used as a loading control and the blot shown is representative of three separate experiments). (B) After 24 and 48 h, PGE_2 production was measured in culture supernatants according to the manufacturer's instructions (PGE_2 EIA Kit, Cayman Chemical). Values are expressed as mean ± SD (*p*-value relative to control group, $^*p < 0.05$). (C) HT-29 cells were pre-treated for 2 h with 10 μM NS-398 before adding 17 μg/mL SN1 or 3.5 μg/mL SN2 for 24 h. Apoptosis was evaluated in the total cell pool lysate by measuring DNA fragmentation. Results were reported as n-fold compared to control. For all experiments each value represents the mean ± SD from three separate experiments ($^*p < 0.05$ vs. *SN1 or SN2 group*).

extrinsic pathway involving cell surface receptors and an intrinsic pathway using mitochondria and the endoplasmic reticulum. Our data showed that SN1 and SN2 induce apoptosis by the intrinsic pathway, since they lead to the cleavage of caspase 9, caspase 3, and PARP, and up-regulating Bax. The ability of p53 to control passage through the cell cycle (in G1 and in G2) and to control apoptosis in response to abnormal proliferative signals and stress including DNA damage is considered to be important for its tumor suppression function. Here, we noticed that SN1 and SN2 up-regulated the expression of p-p53 and p21 and downregulated the expression of Bcl-2 in HT-29 and HCT-116 cells. Thus, SN1 and SN2 induced apoptosis by regulating the expression of apoptosis-related proteins p53, p21, Bcl-2, and Bax.

Genome maintenance activities including DNA repair, cell division cycle control, and checkpoint signaling pathways preserved genome integrity and prevented diseases. Gold(III) porphyrin complexes are known to induce cell cycle arrest which played an important role in the antitumor activity of such drugs. It was reported that gold(III) porphyrin complexes caused cell cycle arrest in ovarian cancer cells in G_0/G_1 phase [42]. In our study, SN1 and SN2 induced significant G2/M arrest in HCT-116 cells. Cyclin-Cdk complexes played a central role in

cell cycle progression. The function of cyclin-Cdks is to run the cell cycle smoothly. Specifically, G_2/M-phase cyclin and G_2/M phase Cdk (cyclin B-Cdk1 complex) function at the start of the M (Mitotic) phase and this complex is the aim of the pathways that cause a cell cycle arrest in the G_2/M phase. Our results are consistent with this data since SN1 and SN2 caused cell cycle arrest in G_2/M phase, and we observed downregulation of the expression of the proteins cyclin B1 and Cdk1 along with up- regulation of the active form of p53, p21 and Bax which may play an early role in cell cycle arrest. This results have revealed a mechanism by which the two gold(III) porphyrin derivatives, SN1 and SN2, induced apoptosis and cell cycle arrest through the regulation of p-p53/p21/Cdk1/cyclin B1 pathway.

In a recent study, a novel mechanism, in which oxidative stress induced phosphorylation of MAPKs and NF-κB and resulted in increased COX-2 expression and PGE_2 synthesis was elucidated [43]. This correlation between COX-2 expression and Akt/ERK/NF-κB survival pathways was also noticed in our results. The three pathways, PI3K/Akt, NF-κB and ERK, are important for cell survival, proliferation, metastasis and angiogenesis and they are deactivated by most chemotherapeutic agents. Here, we showed that SN1 and SN2 lead to decrease in the activity of Akt where the phosphorylated form (p-Akt) decreased with time as well as they caused an important decrease in the phosphorylation of ERK and activity of NF-κB.

Genetic studies demonstrated that deletion of the *COX-2* gene resulted in decreased tumor formation in the small intestine and colon of *ApcMin/+* mice (a mouse model of CRC) [44] and inhibition of endogenous PGE_2 via genetic deletion of microsomal prostaglandin E synthase (mPGES)-1 suppressed intestinal tumorigenesis in *ApcMin/+* and AOM models [45]. Our results have first shown that SN1 and SN2 complexes affected p38/MAPK pathway by increasing p38 phosphorylation then we recorded an increase in the expression of COX-2 and its enzymatic product PGE_2. Moreover, the COX-2 inhibition with NS-398 increased the DNA degradation and intensified the cell death in HT-29 cells. These findings emphasized that p38 regulated COX-2 which played a key role in colorectal carcinogenesis. In addition, HCT-116 cells were more susceptible to treatment than HT-29 cells because of the crucial role of COX-2 in apoptosis resistance [46].

5. Conclusions

In conclusion, we have demonstrated the in vitro effects of SN1 and SN2 in inhibiting proliferation of CRC cell lines HT-29 and HCT-116, through the induction of cellular apoptosis and deactivation of cellular survival pathways. Of significance, the ability of construction of cancer-targeted in vivo delivery nanosystem has given SN1 and SN2 complexes the potentiality of becoming a promising chemotherapeutic agent against CRC.

Supplementary data to this article can be found online at http://dx.doi.org/10.1016/j.jinorgbio.2017.08.024.

Conflict of interest

The authors declare that they have no conflicts of interest with the contents of this article.

Authors contribution

SN, FB and RG synthesized and characterized **SN1** and **SN2** shown in Fig. 1. FD performed and analyzed the experiments shown in Figs. 2 to 10 and wrote the paper. DYL, CFD and VS wrote the paper. MDA and WK contributed for the correction of the paper. BL conceived, designed the experiments and wrote the paper. All authors approved the final version of the manuscript.

Acknowledgements

This research was supported by grants from the French Ministry of Education and Research and from the Lebanese University.

References

[1] L.A. Torre, F. Bray, R.L. Siegel, J. Ferlay, J. Lortet-Tieulent, A. Jemal, CA Cancer J. Clin. 65 (2015) 87–108.
[2] F.A. Haggar, R.P. Boushey, Clin. Colon Rectal Surg. 22 (2009) 191–197.
[3] B. Vogelstein, E.R. Fearon, S.R. Hamilton, S.E. Kern, A.C. Preisinger, M. Leppert, Y. Nakamura, R. White, A.M. Smits, J.L. Bos, N. Engl. J. Med. 319 (1988) 525–532.
[4] S. Tu, R. Wai-Yin Sun, M.C. Lin, J. Tao Cui, B. Zou, Q. Gu, H.F. Kung, C.M. Che, B.C. Wong, Cancer 115 (2009) 4459–4469.
[5] C.A. Rabik, M.E. Dolan, Cancer Treat. Rev. 33 (2007) 9–23.
[6] C.X. Zhang, S.J. Lippard, Curr. Opin. Chem. Biol. 7 (2003) 481–489.
[7] L. Messori, F. Abbate, G. Marcon, P. Orioli, M. Fontani, E. Mini, T. Mazzei, S. Carotti, T. O'Connell, P. Zanello, J. Med. Chem. 43 (2000) 3541–3548.
[8] K.H. Chow, R.W. Sun, J.B. Lam, C.K. Li, A. Xu, D.L. Ma, R. Abagyan, Y. Wang, C.M. Che, Cancer Res. 70 (2010) 329–337.
[9] R.W. Sun, M. Zhang, D. Li, M. Li, A.S. Wong, J. Inorg. Biochem. 163 (2016) 1–7.
[10] L. He, T. Chen, Y. You, H. Hu, W. Zheng, W.L. Kwong, T. Zou, C.M. Che, Angew. Chem. Int. Ed. Eng. 53 (2014) 12532–12536.
[11] L. Cao, X.B. Quan, W.J. Zeng, X.O. Yang, M.J. Wang, J. Cell Death 9 (2016) 19–29.
[12] W. Meikrantz, R. Schlegel, J. Cell, Biochemist 58 (1995) 160–174.
[13] Y. Yao, W. Dai, J. Carcinog. Mutagen. 5 (2014) 1000165.
[14] T. Regad, Cancers (Basel) 7 (2015) 1758–1784.
[15] G.S. Martin, Cancer Cell 4 (2003) 167–174.
[16] D. Wang, R.N. Dubois, Oncogene 29 (2010) 781–788.
[17] A. Greenhough, H.J. Smartt, A.E. Moore, H.R. Roberts, A.C. Williams, C. Paraskeva, A. Kaidi, Carcinogenesis 30 (2009) 377–386.
[18] Z. Zhou, Z. Han, Z.-R. Lu, Biomaterials 85 (2016) 168–179.
[19] G.M.A. Ndong Ntoutoume, R. Granet, J.-P. Mbakidi, F. Brégier, D.Y. Léger, C. Fidanzi-Dugas, V. Lequart, N. Joly, B. Liagre, V. Chaleix, V. Sol, Bioorg. Med. Chem. Lett. 26 (2016) 941–945.
[20] C. Mauriello-Jimenez, J. Croissant, M. Maynadier, X. Cattoën, M. Wong, Chi Man, V. Chaleix, V. Sol, J. Vergnaud, M. Garcia, M. Gary-Bobo, L. Raehm, J.-O. Durand, J. Mater. Chem. B 3 (2015) 3681–3684.
[21] H. Maeda, J. Wu, T. Sawa, Y. Matsumura, K. Hori, J. Control. Release 65 (2000) 271–284.
[22] S. Izumi, Y. Urano, K. Hanaoka, T. Terai, T. Nagano, J. Am. Chem. Soc. 131 (2009) 10189–10200.
[23] E.S. Lee, Z. Gao, Y.H. Bae, J. Control. Release 133 (2008) 164–170.
[24] V.F. Slagt, P.W. van Leeuwen, J.N. Reek, Chem. Commun. 19 (2003) 2474–2475.
[25] C. Fidanzi-Dugas, B. Liagre, G. Chemin, A. Perraud, C. Carrion, C.Y. Couquet, R. Granet, V. Sol, D.Y. Léger, Biochim. Biophys. Acta 1861 (2017) 1676–1690.
[26] B. Ismail, L. Ghezali, R. Gueye, Y. Limami, C. Pouget, D.Y. Leger, F. Martin, J.L. Beneytout, J.L. Duroux, M. Diab-Assaf, C. Fagnere, B. Liagre, Int. J. Oncol. 43 (2013) 1160–1168.
[27] D.Y. Leger, B. Liagre, J.L. Beneytout, Int. J. Oncol. 28 (2006) 201–207.
[28] L. Ghezali, D.Y. Leger, Y. Limami, J. Cook-Moreau, J.L. Beneytout, B. Liagre, Exp. Cell Res. 319 (2013) 1043–1053.
[29] S. Diab, C. Fidanzi, D.Y. Léger, L. Ghezali, M. Millot, F. Martin, R. Azar, F. Esseily, A. Saab, V. Sol, M. Diab-Assaf, B. Liagre, Int. J. Oncol. 47 (2015) 220–230.
[30] C. Lepage, B. Liagre, J. Cook-Moreau, A. Pinon, J.L. Beneytout, Int. J. Oncol. 36 (2010) 1183–1191.
[31] C.M. Che, R.W. Sun, W.Y. Yu, C.B. Ko, N. Zhu, H. Sun, Chem. Commun. 14 (2003) 1718–1719.
[32] C.T. Lum, X. Liu, R.W. Sun, X.P. Li, Y. Peng, M.L. He, H.F. Kung, C.M. Che, M.C. Lin, Acta Oncol. 50 (2011) 719–726.
[33] L. Sun, H. Chen, Z. Zhang, O. Yang, H. Tong, A. Xu, C. Wang, J. Inorg. Biochem. 108 (2012) 47–52.
[34] F. Schmitt, K. Donnelly, J.K. Muenzner, T. Rehm, V. Novohradsky, V. Brabec, J. Kasparkova, M. Albrecht, R. Schobert, T. Mueller, J. Inorg. Biochem. 163 (2016) 221–228.
[35] D. Höfer, H.P. Varbanov, M. Hejl, M.A. Jakupec, A. Roller, M. Galanski, B.K. Keppler, J. Inorg. Biochem. 174 (2017) 119–129.
[36] Y.F. To, R.W. Sun, Y. Chen, V.S. Chan, W.Y. Yu, P.K. Tam, C.M. Che, C.L. Lin, Int. J. Cancer 124 (2009) 1971–1979.
[37] A. Casini, C. Hartinger, C. Gabbiani, E. Mini, P.J. Dyson, B.K. Keppler, L. Messori, J. Inorg. Biochem. 102 (2008) 564–575.
[38] D. Hu, Y. Liu, Y.T. Lai, K.C. Tong, Y.M. Fung, C.N. Lok, C.M. Che, Angew. Chem. Int. Ed. Eng. 55 (2016) 1387–1391.
[39] Y. Wang, Q.Y. He, R.W. Sun, C.M. Che, J.F. Chiu, Cancer Res. 65 (2005) 11553–11564.
[40] C.T. Lum, Z.F. Yang, H.Y. Li, R. Wai-Yin Sun, S.T. Fan, R.T. Poon, M.C. Lin, C.M. Che, H.F. Kung, Int. J. Cancer 118 (2006) 1527–1538.
[41] L. Engman, M. McNaughton, M. Gajewska, S. Kumar, A. Birmingham, G. Powis, Anti-Cancer Drugs 17 (2006) 539–544.
[42] M. Coronnello, E. Mini, B. Caciagli, M.A. Cinellu, A. Bindoli, C. Gabbiani, L. Messori, J. Med. Chem. 48 (2005) 6761–6765.
[43] Y. Onodera, T. Teramura, T. Takehara, K. Shigi, K. Fukuda, FEBS Open Bio 5 (2015) 492–501.
[44] P.C. Chulada, M.B. Thompson, J.F. Mahler, C.M. Doyle, B.W. Gaul, C. Lee, H.F. Tiano, S.G. Morham, O. Smithies, R. Langenbach, Cancer Res. 60 (2000) 4705–4708.
[45] M. Nakanishi, D.C. Montrose, P. Clark, P.R. Nambiar, G.S. Belinsky, K.P. Claffey, D. Xu, D.W. Rosenberg, Cancer Res. 68 (2008) 3251–3259.
[46] C. Jiang, Q. Wang, Z. Xu, W.S. Li, C. Chen, X.Q. Yao, F.K. Liu, Am. J. Cancer Res. 5 (2015) 2012–2021.